Title
GluA1 signal peptide determines the spatial assembly of heteromeric AMPA receptors

Journal
Proceedings of the National Academy of Sciences of the United States of America, 113(38)

ISSN
0027-8424

Authors
He, Xue-Yan
Li, Yan-Jun
Kalyanaraman, Chakrapani
et al.

Publication Date
2016-09-20

DOI
10.1073/pnas.1524358113

Peer reviewed

GluA1 signal peptide determines the spatial assembly of heteromeric AMPA receptors

Xue-Yan He[a,1], Yan-Jun Li[a,1], Chakrapani Kalyanaraman[b], Li-Li Qiu[a,c], Chen Chen[a], Qi Xiao[a], Wen-Xue Liu[a,d], Wei Zhang[e], Jian-Jun Yang[c], Guiquan Chen[a], Matthew P. Jacobson[b], and Yun Stone Shi[a,2]

[a]State Key Laboratory of Pharmaceutical Biotechnology and MOE Key Laboratory of Model Animal for Disease Study, Model Animal Research Center, Nanjing University, Nanjing 210061 China; [b]Department of Pharmaceutical Chemistry, University of California, San Francisco, CA 94158; [c]Department of Anesthesiology, Zhongda Hospital, Medical School, Southeast University, Nanjing 210009, China; [d]Department of Intensive Care Medicine, Zhongda Hospital, Medical School, Southeast University, Nanjing 210009, China; and [e]Institute of Chinese Integrative Medicine, Hebei Medical University, Shijiazhuang 050017, China

Edited by Richard L. Huganir, The Johns Hopkins University School of Medicine, Baltimore, MD, and approved July 25, 2016 (received for review December 10, 2015)

AMPA-type glutamate receptors (AMPARs) mediate fast excitatory neurotransmission and predominantly assemble as heterotetramers in the brain. Recently, the crystal structures of homotetrameric GluA2 demonstrated that AMPARs are assembled with two pairs of conformationally distinct subunits, in a dimer of dimers formation. However, the structure of heteromeric AMPARs remains unclear. Guided by the GluA2 structure, we performed cysteine mutant cross-linking experiments in full-length GluA1/A2, aiming to draw the heteromeric AMPAR architecture. We found that the amino-terminal domains determine the first level of heterodimer formation. When the dimers further assemble into tetramers, GluA1 and GluA2 subunits have preferred positions, possessing a 1–2–1–2 spatial assembly. By swapping the critical sequences, we surprisingly found that the spatial assembly pattern is controlled by the excisable signal peptides. Replacements with an unrelated GluK2 signal peptide demonstrated that GluA1 signal peptide plays a critical role in determining the spatial priority. Our study thus uncovers the spatial assembly of an important type of glutamate receptors in the brain and reveals a novel function of signal peptides.

AMPA receptors | signal peptide | spatial assembly | stoichiometry

Ionotropic glutamate receptors mediate the excitatory neurotransmission in the brain (1). These receptors are homomeric or heteromeric tetramers, which are divided into three groups—NMDA, AMPA, and kainate receptors—based on their binding preference to different agonists. Among them, AMPAR subunits GluA1–4 form heteromeric as well as homomeric receptors. In the brain, the GluA2 mRNA processing an A-to-I conversion results in the replacement of a neutral glutamine residue (GluA2Q) to a positively charged arginine (GluA2R; GluA2 generally refers to this edited isoform) at the pore region (2). This RNA editing significantly changes the biophysical properties of AMPARs containing GluA2 subunits. The receptors containing GluA2R are Ca^{2+}-impermeable and have linear *I–V* curves, whereas receptors without GluA2 are Ca^{2+}-permeable and show strong inward rectifying *I–V* relationships (3, 4). In recombinant expression systems, GluA1, GluA3, and GluA4 prefer to coassemble with GluA2 to form heteromeric receptors, whereas they do form homomeric receptors in the absence of GluA2 (5-8). GluA2-containing receptors are dominant in the brain, particularly in the pyramidal neurons (9). In hippocampal CA3–CA1 synapses, the GluA1/A2 is the major component of AMPARs, whereas GluA2/A3 contributes to a lesser amount (9, 10).

How the heteromeric AMPARs are assembled is intriguing. Biochemical and functional studies have revealed that AMPARs are tetrameric assemblies (11–13). Biophysical studies have suggested that GluA1 and GluA2 might randomly assemble into heteromers so that all of the 3:1, 2:2, or 1:3 stoichiometries can form, depending on the relative abundance of each subunits (14), or the fixed 2:2 stoichiometry is preferred (5, 15). However, direct evidence of how heteromeric AMPARs are assembled is lacking, and the architectures of heteromeric AMPARs remain unclear.

Recently, high-resolution X-ray structures of ionotropic glutamate receptors have provided1 detailed conformational information on these receptors. The X-ray crystal structure of GluA2 homomers demonstrates that the receptors have a twofold symmetry (16–18), with two pairs of conformationally distinct subunits. Viewed at the amino-terminal domain (ATD) level, the A-type conformation represents the subunits away from the symmetric axis, and the B-type conformation represents the subunits proximal to the symmetric center, suggesting that GluA2 homomers are thus arranged in an A–B–A′–B′ architecture (16–18). The structure of heteromeric NMDA-type glutamate receptor (GluN1/N2B) also shows a twofold symmetry, with GluN1 at the A positions and GluN2B at the B positions in a 1–2–1–2 (GluN1–GluN2–GluN1–GluN2) fashion (19). The ATD structure of heteromeric kainate receptors (GluK2/K5) shows similar architecture, with GluK5 at the A positions and GluK2 at the B positions (20). Thus, it is suspected that the heteromeric AMPARs might possess a similar symmetry to NMDAR and kainate receptors.

Here, we used disulfide-bond cross-linking experiments to establish the GluA1/A2 heteromeric AMPAR assembly. We found that GluA1/A2 prefers to form 2:2 stoichiometry with 1–2–1–2 (GluA1–GluA2–GluA1–GluA2) architecture, which was mainly determined by the amino-terminal excisable signal peptides (SPs). Furthermore, replacements with an unrelated GluK2 SP revealed

Significance

In the brain, AMPA-type glutamate receptors, especially heteromeric GluA1/A2s, are the major postsynaptic receptors mediating fast excitatory neurotransmission. Recently, the crystal structure of GluA2 homomeric AMPA-type glutamate receptors (AMPARs) revealed some interesting features, such as the four subunits in each AMPAR are of two different conformations. However, what the heteromeric GluA1/A2 receptors look like is unknown. In this study, we used a biochemical technique called cysteine cross-linking assay to analyze the spatial architecture of GluA1/A2s. We determined that GluA1/GluA2s have preferred spatial assembly. Surprisingly, this spatial assembly pattern is dictated by the excisable signal peptides, but not the intrinsic sequences of the subunit proteins.

Author contributions: Y.S.S. designed research; X.-Y.H., Y.-J.L., L.-L.Q., C.C., W.-X.L., and Y.S.S. performed research; C.C. established models; X.-Y.H., Y.-J.L., C.K., C.C., Q.X., W.Z., J.-J.Y., G.C., M.P.J., and Y.S.S. analyzed data; and X.Y.-H. and Y.S.S. wrote the paper.

The authors declare no conflict of interest.

This article is a PNAS Direct Submission.

[1]X.-Y.H. and Y.-J.L. contributed equally to this work.

[2]To whom correspondence should be addressed. Email: yunshi@nju.edu.cn.

This article contains supporting information online at www.pnas.org/lookup/suppl/doi:10.1073/pnas.1524358113/-/DCSupplemental.

that the SP of GluA1 played a major role in determining AMPAR spatial assembly. This work uncovered the architecture of GluA1/A2 AMPARs in the brain and revealed a novel function of SPs for transmembrane proteins.

Results

GluA1 and GluA2 Form Heterodimers in ATDs. The crystal structures of homotetrameric GluA2 demonstrate that AMPARs are assembled with two pairs of conformationally distinct subunits (16–18). The different subunit conformations in the AMPAR complex further increase the assembly complexity of heteromeric AMPARs. Regarding GluA1/A2 receptors, if GluA1 and GluA2 can be randomly assembled, there would be eight different possible spatial arrangements (Fig. S1). For example, a receptor composed of one GluA1 and three GluA2s (1:3 stoichiometry) would have two possible architectures, such as 1–2–2–2 (with GluA1 in the A-type conformation) and 2–1–2–2 (with GluA1 in the B-type conformation) (Fig. S1*A*). Similarly, there would be two assembly possibilities for a receptor with 3:1 stoichiometry (Fig. S1*B*). If the receptor prefers to assemble in 2:2 stoichiometry (15), there would be four differential spatial arrangements (Fig. S1*C*). Even if the receptor has a fixed 2:2 stoichiometry and the preferred spatial symmetry (5), it still could be assembled into 1–2–1–2 or 2–1–2–1 architecture.

To understand the assembly of heteromeric GluA1/A2 receptors, we built a model of homomeric GluA1 receptors based on the X-ray structure of homomeric GluA2 AMPAR [Protein Data Bank identifier (PDB ID) 3KG2; ref. 18 and Fig. 1*A*]. The structure of the GluA1 model was Y-shaped, with four subunits presenting two different conformations in the tetramer, arranged in A–B–A′–B′ architecture (Fig. 1 *A* and *B*). Both ATD and ligand-binding domain (LBD) assembled as dimer of dimers. Notably, the subunit pairs that form the ATD dimer swapped partners in the LBD.

To experimentally verify the dimer formation in ATDs and LBDs in our GluA1 model, we generated a series of cysteine mutants of GluA1 and GluA2 and tested the oligomer formation by nonreducing Western blot assays. The wild-type (WT) GluA1 contains 13 native cysteine residues, which might interfere with the introduced cysteines by forming spontaneous cross-linking background bands (Fig. S2*A*). According to the GluA1 model, Cys-57 and -305 in the ATD and Cys-714 and -769 in the LBD probably form native disulfide bonds, and Cys-93, -89, -186, and -421 are buried in the protein interior. The remaining five cysteine residues, including Cys-524, -585, -811, -825, and -875, were mutated to nonreducing alanines. As expected, the mutated GluA1 (GluA1m) showed reduced background on the nonreducing Western gel (Fig. S2*A*). Similarly, we generated a mutated GluA2 (GluA2m) in which four surface cysteine residues,

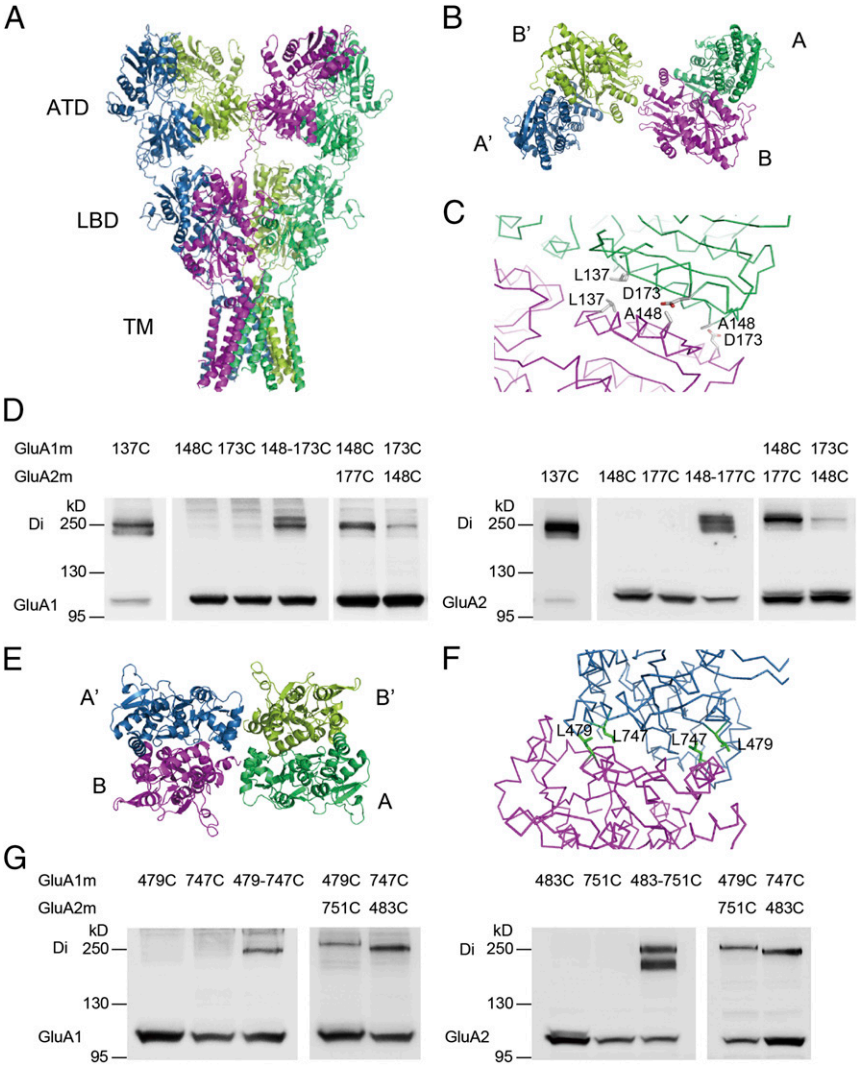

Fig. 1. Heteromeric dimers in the ATD and LBD of GluA1/A2 receptor. (*A*) Homomeric GluA1 model with the four subunits colored individually. (*B* and *C*) Cartoon diagram for the view from the top of ATD (*B*) and close-up of the interface between subunits A and B (*C*) showing the positions cysteine mutants were introduced to cross-link the A and B subunits in a tetramer assembly. (*D*) Western blot for GluA1 and GluA2 ATD cross-links created by cysteine mutagenesis designed in *C*. (*E* and *F*) Cartoon diagram for the view from the top of LBD (*E*) and stereoview (*F*) showing cysteine mutants designed to cross-link the B and A′ subunits in a GluA1/A2 tetramer assembly. (*G*) Western blot for GluA1 and GluA2 LBD cross-links created by cysteine mutagenesis designed in *F*.

Cys-436, -528, -589, and -815, were mutated to alanine residues. The GluA2m had a reduced background, as expected (Fig. S2*B*). These two mutants were functional with the same biophysical properties as WT receptors. The *I–V* curves were strongly rectified for GluA1m and linear for GluA1m/A2m (Fig. S2 *C* and *D*). Therefore, all of the following experiments were based on these mutated forms of GluA1 and GluA2.

The ATD of GluA1 model forms a dimer of dimers like that of the GluA2 template (Fig. 1*B*). The ATDs of subunit A and B (and so for A′ and B′) interact with a hydrophobic area, forming the first level of dimer (Fig. 1 *B* and *C*). The C_α atoms of Leu-137 residues in subunit A and B are at the distance of ∼8.1 Å, optimal for spontaneous formation of a disulfide bond (Fig. 1*C*). Introduction of a cysteine residue at this position led to the formation of a dimer band at ∼250 kDa on the nonreducing Western gel (Fig. 1*D*). Similarly, introduction of a cysteine at the corresponding site in GluA2 (GluA2m_L137C) also showed a dimer band (Fig. 1*D*). In the GluA1 model, residue Ala-148 in subunit A is close to residue Asp-173 in subunit B at the distance of 6.1 Å between two C_α atoms, whereas residue Ala-148 in subunit B is close to residue Asp-173 in subunit A at the distance of 5.5 Å (Fig. 1*C*). In addition, the distance between the two Ala-148 residues and two Asp-173 residues in subunits A and B is too far to form a disulfide bond. To examine whether GluA1 and GluA2 could form heterodimers at the amino-terminal interface of subunit A–B, we introduced these cysteine mutations in GluA1 and GluA2. We found that GluA1m_A148C alone or GluA1m_D173C alone only showed monomer bands, whereas double mutations showed a dimer band (Fig. 1*D*). Similar results were seen in GluA2m, where the disulfide band could be formed between residues GluA2m_A148C and GluA2m_D177C (Fig. 1*D*). Additionally, a heterodimer could be detected both when GluA1m_A148C were coexpressed with GluA2m_D177C and when GluA1m_D173C coexpressed with GluA2m_A148C (Fig. 1*D*). Therefore, heterodimers could be formed in the ATDs of GluA1/A2 receptors.

GluA1 and GluA2 Form Heterodimers in LBDs. To examine whether heterodimers would also form in the LBD, in which subunit A and B′ (A′ and B) would make pairs, we chose residues Leu-479 and -747 as candidates that could form a disulfide band in the model (Fig. 1*E*). The C_α atom of residue Leu-479 in subunit A′ is close to that of the Leu-747 residue in subunit B at the distance of 5.6 Å, and the C_α atom of residue Leu-479 in subunit B is close to that of the Leu-747 residue in subunit A′ at the distance of 5.6 Å (Fig. 1*F*). However, the Leu-479 residues in A′ and B are far from each other, and so are the Leu-747 residues. According to our nonreducing Western analyses, the high-molecular-mass dimer band was only shown in GluA1m_L479C_L747C double mutations, but not in the GluA1m_L479C or GluA1m_L747C single mutant (Fig. 1*G*). The corresponding pair of L483C and L751C in GluA2m showed a similar dimer band. In addition, coexpression of GluA1m_L479C and GluA2m_L751C formed a heterodimer band, as did coexpression of GluA1m_L747C and GluA2m_L483C (Fig. 1*G*). Collectively, a heterodimer could be formed in the LBDs of GluA1/A2 receptors.

GluA1 and GluA2 Have Preferred Positions in Tetrameric Assemblies. Thus far, we have demonstrated heterodimer formation in the ATD and LBD of GluA1/A2 receptors. However, how do the heterodimers assemble into a tetramer? Does GluA1 (or GluA2) prefer to localize to subunit A (A′) or B (B′)? We therefore examined the interface between dimers. In between ATD dimers of the GluA2 homotetramer, subunits B and B′ interact with each other (around Val-209), whereas in between LBD dimers, subunits A and A′ interact with each other (around Ile-664) (18). We introduced cysteine residues at these interfaces of GluA1 and GluA2 and found that the spontaneous cross-linking between LBD dimers (A1m_I660C and A2m_I664C; Fig. 2 *A–C* and Fig. S3 *C* and *D*) was much stronger and clearer than between ATD dimers (A1m_G205C and A2m_V209C in Fig. S3 *A* and *B*). Thus, further experiments with coexpression of GluA1 and GluA2 were carried out with the mutations at the LBD interface. We reasoned that, if GluA1 prefers to assemble into the A (and A′) positions and GluA2 prefers the B (B′) positions, then coexpression of GluA1m_I660C with GluA2m would still generate a GluA1 dimer band. Indeed, when GluA1m_I660C was coexpressed with the same amount of or up to four times as much GluA2m, high-molecular-mass bands corresponding to dimer size were constantly detected on the nonreducing Western gel (Fig. 2*B*). Interestingly, increasing GluA2m amount in the expression system only slightly, but not significantly, reduced the dimer band strength (Fig. 2 *B*, *Lower*, shows the quantification), suggesting that GluA1 sticks to position A and A′ in heteromeric GluA1/A2 receptors [the rectification indexes (RIs) indicating linear *I–V* curves; Table S1]. We further analyzed coexpression of GluA2m_I664C with GluA1m and found that the addition of GluA1 sharply reduced the GluA2 dimer band strength (Fig. 2*C*). The 1:1 ratio coexpression reduced the dimer band strength to ∼30%. With a 1:2 and 1:4 ratio, the GluA2 dimer bands almost disappeared, suggesting that GluA2 prefers to locate on position B (B′). A theoretical comparison between 1–2–1–2, 2–1–2–1 and random assembly demonstrated that the 1–2–1–2 assembly model can best fit our data for coexpression of GluA1 and GluA2 (*Discussion*). Therefore, these data indicate that the heteromeric AMPARs have a preferred 2:2 stoichiometry and assemble into a 1–2–1–2 conformation (Fig. 2*I*).

We noticed that the total GluA2m_I664C expression (dimer plus monomer) appeared to decrease when coexpressed with GluA1m with a nonreducing Western assay (Fig. 2*C*), which might complicate the interpretation of our results. However, after dimers disassembled by DTT, the expression levels of GluA2 were constant (Fig. S3*F*), suggesting that the apparent expression change in the absence of DTT was due to higher sensitivity of antibody to dimers. The GluA1 antibody was also more sensitive to dimers, and GluA1 expression was not affected by coexpression of GluA2 (Fig. S3*E*). Furthermore, the whole-lysed receptor proteins used in our experiments contained the immature dimer or monomer intermediate, which might interfere with our cross-linking bands. We thus biotinylated and isolated the surface mature receptors and analyzed their cross-linking patterns (Fig. S4). The results were the same as whole-lysed receptors, suggesting that the immature intermediates contribute little to the receptor pool under our experimental conditions.

The spontaneous disulfide band formation between the A–A′ interface in LBD reduces the maximal channel opening in AMPAR GluA2Q (18) and kainate receptor GluK2 (21). We wondered whether this is the case for heteromeric AMPARs. In the presence of the AMPAR desensitization blocker trichloromethiazide (TCM), the glutamate-induced currents of GluA1m_I660C were significantly enhanced by reducing reagent DTT, whereas the currents of GluA1m were not (Fig. S5 *A* and *B*). The GluA2 with arginine in the pore has little currents in HEK cells; therefore, we made GluA2Qm by mutating the arginine residue to glutamine. The glutamate-induced currents of GluA2Qm were insensitive to DTT, whereas those of GluA2Qm_I664C were significantly enhanced by DTT (Fig. S5 *C* and *D*), consistent with the previous report (18). In addition, in the presence of transmembrane AMPAR regulatory proteins (TARPs), the GluA2R could have significant currents (22). We found in the presence of the prototypical TARP γ-2, the GluA2Rm_I664C currents were significantly increased by DTT (Fig. S5 *E* and *F*). Then, we tested the glutamate currents of heteromeric receptors. GluA1m_I660C/GluA2m currents were significantly enhanced by DTT, whereas GluA1m/GluA2m_I664C currents were insensitive (Fig. 2 *D–F*). These data further supported the notion

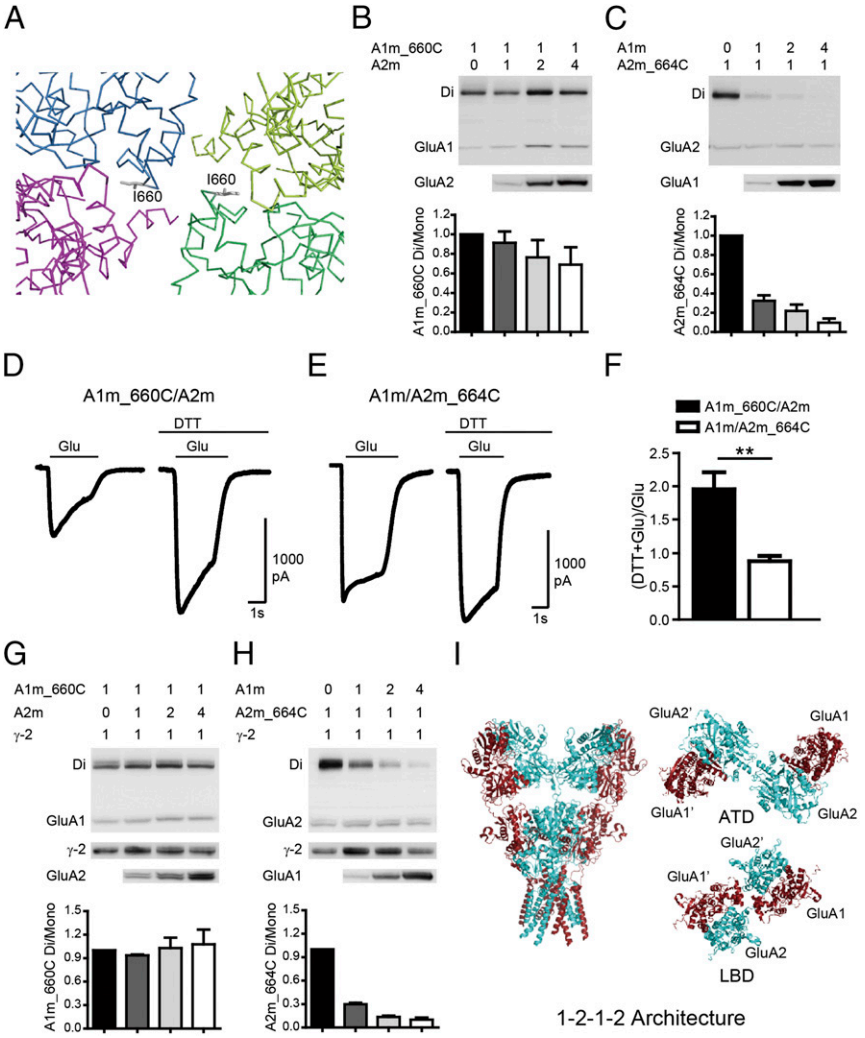

Fig. 2. GluA1 and GluA2 have preferred positions in tetrameric assemblies. (*A*) Stereoview showing cysteine mutants designed to cross A and A′ subunits in a LBD tetramer assembly, with each subunit colored the same as for the GluA1 tetramer shown in Fig. 1. (*B*) The GluA1m_I660C mutation showed spontaneous disulfide-bond formation. Quantifications of ratio between the dimer to the monomer band indicated GluA1 in the A conformation. (*C*) Spontaneous cross-link in GluA2m_I664C mutation was diminished by coexpression with GluA1m. Quantifications of ratio between the dimer to the mono band indicated GluA2 in the B conformation. (*D–F*) The glutamate-induced currents were enhanced by DTT in the GluA1m_I660C/GluA2m channel ($n = 8$), but not in the GluA1m/GluA2m_I664C channel ($n = 8$). Values are means ± SEMs. $^{**}P < 0.01$ (*t* test). (*G* and *H*) AMPAR subunits TARP γ-2 did not change heterotetrameric AMPAR assembly. (*I*) Model of heteromeric AMPARs with a preferred 2:2 stoichiometry and assemble into 1–2–1–2 conformation.

that, in the heteromeric GluA1/A2 receptor, the dimer of dimers interface in LBDs is between GluA1 subunits.

TARP γ-2 Does Not Change the Heterotetrameric AMPAR Architecture. AMPARs are modulated by auxiliary subunits in the brain, including TARPs, cornichons, GSG1L, SynDIG1, CKAMP44, and other proteins (23–28). Among them, TARPs are reported to affect AMPAR synthesis, maturation, trafficking, and function (29). To investigate whether TARPs participate in determining the stoichiometry and assembly of heteromeric AMPARs, we cotransfected TARP γ-2 with GluA1 and GluA2 mutants. In the presence of γ-2, the GluA1m_I660C and GluA2m still cross-linked to form dimer bands, whereas GluA2m_I664C and GluA1m had diminished dimer bands (Fig. 2 *G* and *H*), similar to the results without γ-2 (Fig. 2 *B* and *C*). It should be noted that, without TARP γ-2, the GluA1m_I660C dimer bands slightly decreased with the coexpression of GluA2m, whereas they were more stable with γ-2 (quantification in Fig. 2*B* compared with Fig. 2*G*), indicating that TARP γ-2 might enforce the spatial assembly priority of heteromeric AMPARs with 1–2–1–2 architecture.

The Amino-Terminal Sequences Determine the Spatial Priority of Heteromeric AMPAR Assembly. According to previous reports, ATDs could affect AMPAR assembly (11, 30–33). To determine whether ATDs play a role in determining AMPAR spatial assembly, we made chimeric construct of GluA1–2 by linking GluA1 amino-terminal sequence (ATS; ATD plus SP) to the LBD of GluA2m, and GluA2-1 by fusing the ATS of GluA2 to the LBD of GluA1m. When GluA2-1_I660C was coexpressed with GluA1-2, the GluA1 dimer bands were significantly diminished, whereas GluA1-2_I664C and GluA2-1 showed relatively constant GluA2 dimer bands (Fig. 3 *A* and *B*), indicating that the dimer of dimers interface in LBDs is now between GluA2 subunits. Consistent with the Western data, DTT enhanced the glutamate currents of GluA1-2_I664C/GluA2-1, but not that of GluA2-1_I660C/GluA1-2 (Fig. 3 *E–G*). The dimer bands of GluA1_2-I664C were further stabilized by TARP γ-2 when coexpressed with GluA2-1 (Fig. 3 *C* and *D*).

To identify the specific domains in ATDs contributing to AMPAR assembly, we switched only the ATD interface (AIF) between two subunits to construct GluA1_AIF2 and GluA2_AIF1 (Fig. S6*A*). However, this interchange of AIFs resulted in an unaffected assembly pattern with 1–2–1–2 architecture (Fig. S6 *B* and *C*).

Collectively, swapping the ATSs of GluA1 and GluA2 altered the spatial assembly of the downstream structure (Fig. 3*H*), but the determining domain is not the AIFs in ATDs.

Switching SPs Reverses the Architecture of GluA1/A2. We then only switched the SPs to construct SP2_GluA1 (GluA2 SP fused to GluA1) and SP1_GluA2 (GluA1 SP fused to GluA2), respectively. The dimer bands of SP2_GluA1_I660C were significantly diminished with the coexpression of SP1_GluA2, whereas

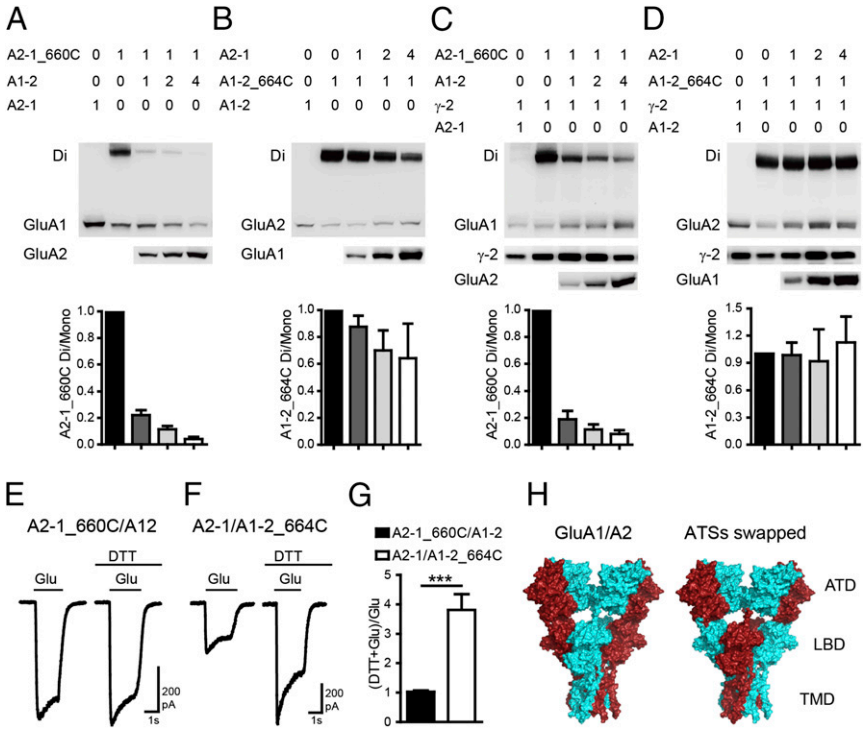

Fig. 3. ATSs determine the spatial priority of heteromeric AMPAR assembly. (*A*) The dimer bands of GluA2-1_I660C were greatly reduced when coexpressed with GluA1-2. (*B*) GluA1-2_I664C showed constant GluA2 dimer band with GluA2-1. (*C* and *D*) GluA2-1 and GluA1-2 have the same preferred positions in tetramer as shown in *A* and *B*, with coexpression of AMPAR subunits TARP γ-2. (*E*–*G*) The glutamate-induced currents were significantly enhanced by DTT only in the GluA2-1/GluA1-2_I664C channel ($n = 7$). Values are means ± SEMs. ***$P < 0.001$ (*t* test). (*H*) Molecular surface view showing that swapping the ATSs of GluA1 and GluA2 alters the spatial assembly.

SP1_GluA2_I664C maintained relatively stable dimer bands with the coexpression of SP2_GluA1 (Fig. 4 *A* and *B*). This pattern was maintained in the presence of TARP γ-2 (Fig. 4 *C* and *D*). DTT-enhancing experiments further demonstrated that the disulfide bond was now formed between GluA2 LBDs (Fig. 4 *E* and *F*). Thus, swapping SPs changed the architecture of GluA1/A2 into 2–1–2–1 (Fig. 4 *G* and *H*). The SPs are not shown in our structure models of AMPARs; we therefore checked the first amino acids in our models where the SPs should link. The positions of the first residues of GluA1s and GluA2s in the WT GluA1/A2 model (Fig. 4*I*) are clearly different. Briefly, the two GluA1_Asn5s, the first amino acids of GluA1s at the A and A′ positions, are at the distance of 125 Å, and the corresponding GluA2_Asn4s are at the distance of 93 Å. In addition, the GluA1_Asn5s is ∼6 Å closer to the cell membrane than GluA2_Asn4s in the model (Fig. 4*I*).

Generally, after guiding newly synthesized peptides to enter the endoplasmic reticulum (ER) during translation, SPs are cleaved off and are absent in mature proteins (34, 35). However, $CRF_{2(a)}R$, a subtype of corticotropin-releasing factor receptors, contains a pseudo-SP that is not removed in the ER (36). To test the fate of SPs in AMPARs, we inserted a FLAG epitope before or after the SPs of GluA1 (Fig. 5*A*) and GluA2. When inserted after GluA1 SP, the expression of FLAG could be detected readily and colocalized with GluA1 (Fig. 5 *B* and *C*). Conversely, when inserted before the SP, the expression of FLAG was barely detectable, whereas the expression of GluA1 was normally detected, indicating that FLAG was removed together with the SP. Insertion of the FLAG epitope before and after GluA2 SP indicated that the GluA2 SP was also excised in the ER (Fig. 5*C*).

The FLAG tag insertion around the SPs had some effects on the AMPAR expression level (Fig. 5 *D* and *E*). FLAG insertion after the SP excising site enhanced their protein level, whereas insertion before the SP inhibited their expression. Swapping SPs had little effect on protein expression level. In addition, GluA1 and GluA2 were undetectable on Western gels when SPs were deleted, demonstrating that SPs are required for AMPAR expression. These data are consistent with the general concepts of N-terminal SP for membrane proteins (34, 35). We also wondered whether Flag insertion affected the spatial assembly of GluA1/A2. When the FLAG epitope was inserted after excising the site of the SP, the dimer band pattern was the same as GluA1/A2 (Fig. S7 *A* and *B*; compare with Fig. 2). When the FLAG epitope was inserted before SP, the dimer band of both GluA1 and GluA2 decreased with coexpression of the other subunit (Fig. S7 *C* and *D*), suggesting that, under this situation, the GluA1 and GluA2 might assemble in a random manner (see theoretical models in Fig. S9).

The SP of GluA1 Determines the Architecture of Heteromeric Receptors. To examine which SP, of GluA1 or of GluA2, is critical in determining the spatial assembly of GluA1/A2, we replaced the SP of GluA1 [18 amino acids (aa)] and GluA2 (21 aa) with an unrelated SP of GluK2 receptor (31 aa), respectively (Fig. 6*A*). The dimer bands of SPK_GluA1m_I660C (SP of GluK2 replacing that of GluA1) were greatly diminished when coexpressed with GluA2m (Fig. 6*B*); the GluA2_I664C dimer bands were also greatly reduced when coexpressed with SPK_GluA1m (Fig. 6*C*). The linear *I*–*V* curve of SPK_GluA1m/GluA2 indicated that the heteromeric receptors were still preferentially formed (Fig. 6*D*). Indeed, the *I*–*V* curve was still linear, even when both GluA1 and GluA2 SPs were replaced with that of GluK2 (Fig. 6*E*). Therefore, when SP of the GluA1 subunit was replaced with an unrelated one, the heteromeric receptor lost spatial priority.

In contrast, when the GluA2 SP was replaced with the GluK2 SP, the dimer bands of GluA1_I660C were relatively stable when coexpressed with SPK_GluA2m, whereas the dimer bands of

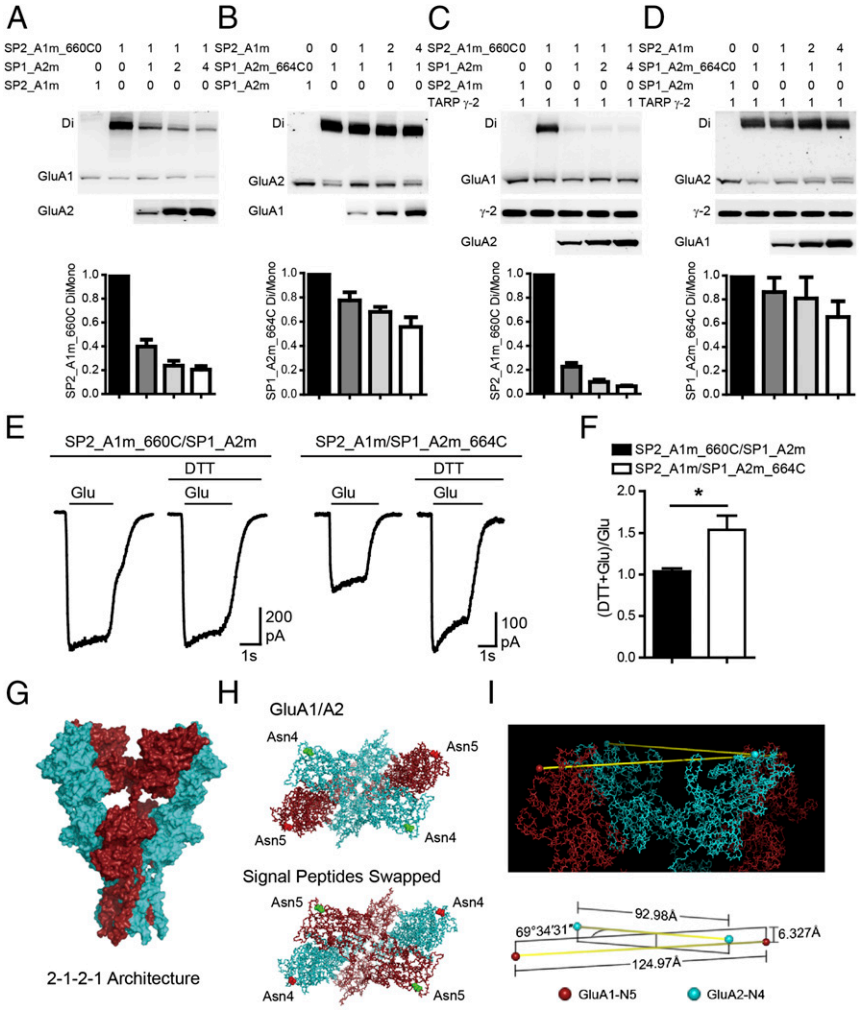

Fig. 4. SPs determine the heteromeric AMPAR assembly. (*A* and *B*) The dimer bands of SP2_A1m_660C were greatly reduced when coexpressed with SP1_GluA2m, whereas SP1_A2m_664C showed a constant GluA2 dimer band with SP2_GluA1m. (*C* and *D*) SP2_GluA1 and SP1_GluA2 have the same preferred positions in the tetramer as shown in *A* and *B*, with coexpression of TARP γ-2. (*E* and *F*) The glutamate-induced currents were significantly enhanced by DTT only in the SP2_A1m/SP1_A2m_664C channel ($n = 10$). Values are means ± SEMs. $^*P < 0.05$ (*t* test). (*G*) Side view of GluA1/A2 with 2–1–2–1 assembly. (*H*) Top view of GluA1/A2 in 1–2–1–2 architecture (*Upper*) and SP swapped GluA1/A2 in 2–1–2–1 architecture (*Lower*). The first amino acids of GluA1 and GluA2 are highlighted. The residues in red link with GluA1 SP. The residues in green link with GluA2 SP. (*I*) Close-up of the first residues of WT GluA1/A2 model in 1–2–1–2 architecture. *Lower* depicts space relationships among the four C_α atoms of GluA1_Asn5s and GluA2_Asn4s. The distance between GluA1_Asn5s is ∼125 Å. The distance between GluA2_Asn4s is ∼93 Å. The line that links GluA1_Asn5s is perpendicular to the symmetric axis, and so is that linking GluA2_Asn4s. The GluA1_Asn5 line is ∼6 Å proximal to membrane relative to GluA2_Asn4 line.

SPK_GluA2_I664C were greatly decreased with the coexpression of GluA1m (Fig. 6 *F* and *G*), indicating an unaffected 1–2–1–2 architecture. Conversely, when the GluA1 SP was replaced with SPK and the GluA2 SP was replaced with GluA1 SP, the heteromeric receptor displayed a preferred 2–1–2–1 architecture (Fig. 6 *H* and *I*). Furthermore, when both the GluA1 and GluA2 were guided by the SP of GluK2 (Fig. S8 *A* and *B*) or GluA1 (Fig. S8 *C* and *D*), neither GluA1 nor GluA2 dimer bands were stable, whereas their *I–V* curves were linear (Table S1).

Together, these findings show that the SP of GluA1 alone is essential for guiding the spatial assembly priority of GluA1/A2 heteromeric AMPAR.

The ATDs Are Critical for the Heteromerization of GluA1/A2. Previous studies have shown that AMPARs in the absence of ATDs retain channel activity (37, 38). To explore the stoichiometry and assembly of GluA1/A2 with the truncation of ATDs, we generated a GluA1ΔN mutant by removing the sequence between Asn-5–Ala-379 and the GluA2ΔN mutant by deleting Asn-4–Leu-381. The glutamate currents of GluA1ΔN in the presence of TCM were strongly rectified (Fig. 7*A*). However, when GluA1ΔN and GluA2ΔN was coexpressed in a 1:1 ratio, the glutamate currents were partially rectified (Fig. 7*B*), suggesting that both homomeric GluA1 receptors and heteromeric GluA1/A2 receptors were formed. Although GluA2ΔN was increased to four times of GluA1ΔN, the *I–V* curve was rather linear, like that of GluA1/A2 (Fig. 7 *C* and *D* and Fig. S2*D*). Therefore, the GluA1 and GluA2 without ATDs lose the priority to heteromerize.

Discussion

Guided by the crystal structure of homomeric GluA2 receptor, we performed cysteine cross-linking experiments to study the stoichiometry and assembly of GluA1/A2 receptors. The GluA1/A2 receptor forms heterodimers in both ATDs and LBDs, which then assemble into heterotetramers, consistent with the dimer-of-dimers theory (5, 33). The spatial assembly of the heterotetramers is consistent with the diagonal spatial arrangement in an early study (5). In addition, we demonstrate that the receptor prefers to assemble as a 1–2–1–2 architecture (Fig. 2*I*), which is mainly determined by the amino-terminal excisable SP of GluA1.

According to the dimer-of-dimers theory, the process of AMPAR assembly could be at least divided into two steps: The subunit peptides first assemble to form dimers, which further dimerize to form tetramers in the second step (5, 33). Our data demonstrate that the heterodimers is preferred in the first step of the assembly. This preference appears to be an intrinsic property of GluA1 and GluA2 sequences because changing SPs do not affect the linear *I–V* curves. Previous studies demonstrated that heterodimers could be formed both in isolated ATDs of GluA2 and GluA3 (39, 40) and in kainate receptors (20, 41). The velocity sedimentation study of isolated ATDs shows that the heterodimer of GluA1/A2 ATDs has the smallest dissociation constant (K_d); thus, the heterodimers are preferred (31). In our study, ATDs form heterodimers in the full-length GluA1/A2. GluA1 and GluA2 without ATD losing the heteromerization

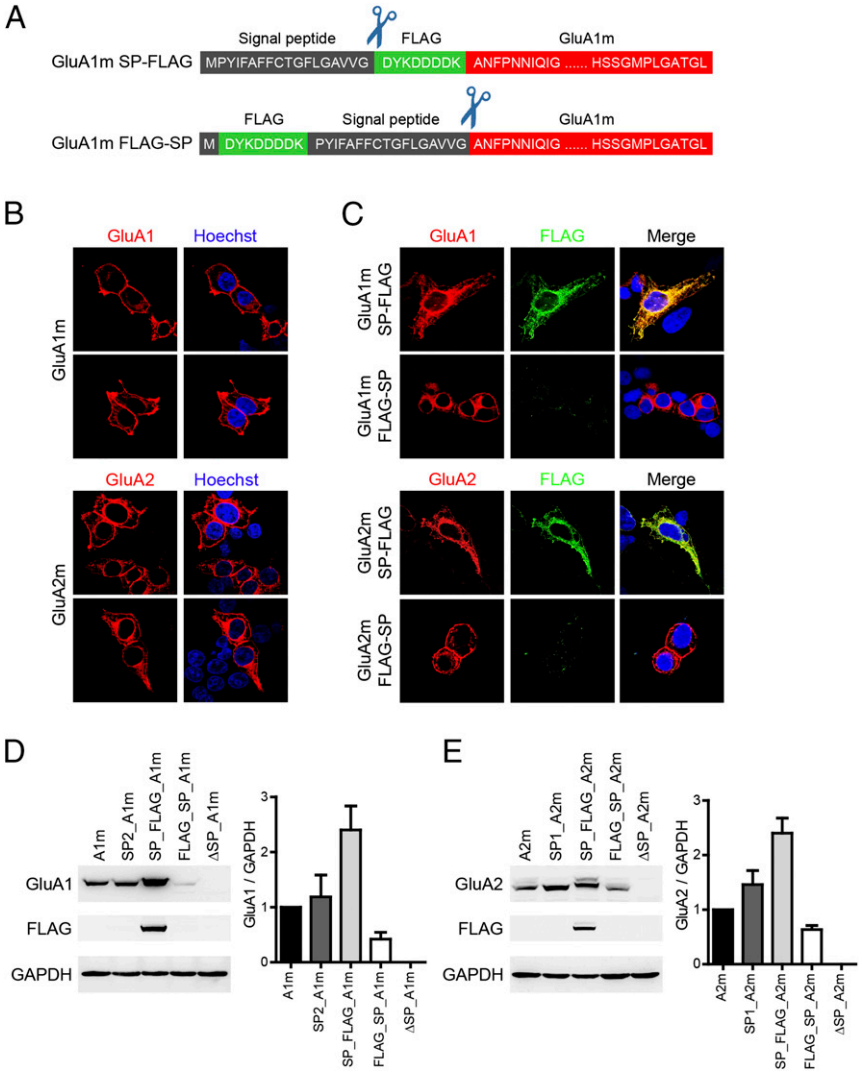

Fig. 5. SPs were cleaved off after AMPAR translation. (*A*) Schematic representation of the constructs. The FLAG tag (green box) was inserted either behind the amino-terminal SP (black box) or behind the starting methionine residue. (*B*) Representative immunofluorescence staining for GluA1 (red) and GluA2 (red) in transfected HEK 293T cells with a GluA1m or GluA2m construct, respectively. Nuclei were stained with Hoechst 33258 (blue). (*C*) Representative immunofluorescence staining for GluA1 (red) and FLAG (green) in transfected HEK 293T cells with GluA1m SP-FLAG or GluA1m FLAG-SP construct designed in *A*, respectively. Nuclei were stained with Hoechst 33258 (blue). (*D* and *E*) Relative expression level of GluA1 (*D*) and GluA2 (*E*) when manipulations were carried out around SP.

priority, supporting the notion that the ATDs are critical for the first step of heterodimerization (11, 31, 33).

In our study, LBDs also form heterodimers in the full-length GluA1/A2. However, in ATD-truncated GluA1ΔN/GluA2ΔN (Fig. 7), the *I–V* curves suggest that heteromeric receptors are not preferred. Therefore, the LBD dimerization should be secondary to ATD dimerization. It has been proposed that, during the first level of dimerization, not only the ATDs, but also the LBDs dimerize between the same pair of subunits (42). However, the LBD dimers have to be loose enough to disperse and reassemble into switched dimerization partners during the second step of dimerization (42).

The second step of assembly, the dimerization of dimers, determines the spatial arrangement of heteromeric GluA1/A2 receptors. The small interface between LBD dimers is suitable for understanding the spatial arrangement of heterotetrameric AMPARs. Introducing cysteine residues at the interface (GluA1m_I660C and GluA2m_I664C) results in clear and strong cross-linking bands in homemeric receptors. Because only receptors with both A-type subunits carrying cysteine residues are able to cross-link, the location information of Cys-tagged subunits can be deduced by analyzing the cross-linking patterns. Clearly the subunits that preferred to locate at A-type positions would have constantly high cross-linking bands, and the subunits that preferred to locate at B-type positions would have diminished dimer bands in coexpression experiments. If the subunits are assembled in a random manner, the cross-linking bands of both subunits would decrease. Thus, three simple models (1–2–1–2, 2–1–2–1, and random) are proposed, and their cross-linking dimer patterns are predicted (Fig. S9*A*). Indeed, we found that these three types of patterns can all happen by manipulating the amino-terminal SPs. GluA1 coexpression with GluA2 either guided by SP2 or SPK has a 1–2–1–2 type of cross-linking pattern. SP1_GluA2 coexpression with GluA1 guided by SP2 or SPK has a 2–1–2–1 type of cross-linking pattern. In the other five conditions, when both subunits are guided by identical SPs or without the SP of GluA1, the receptors are likely assembled in a random model. For these five conditions, because these receptor subunits have intact

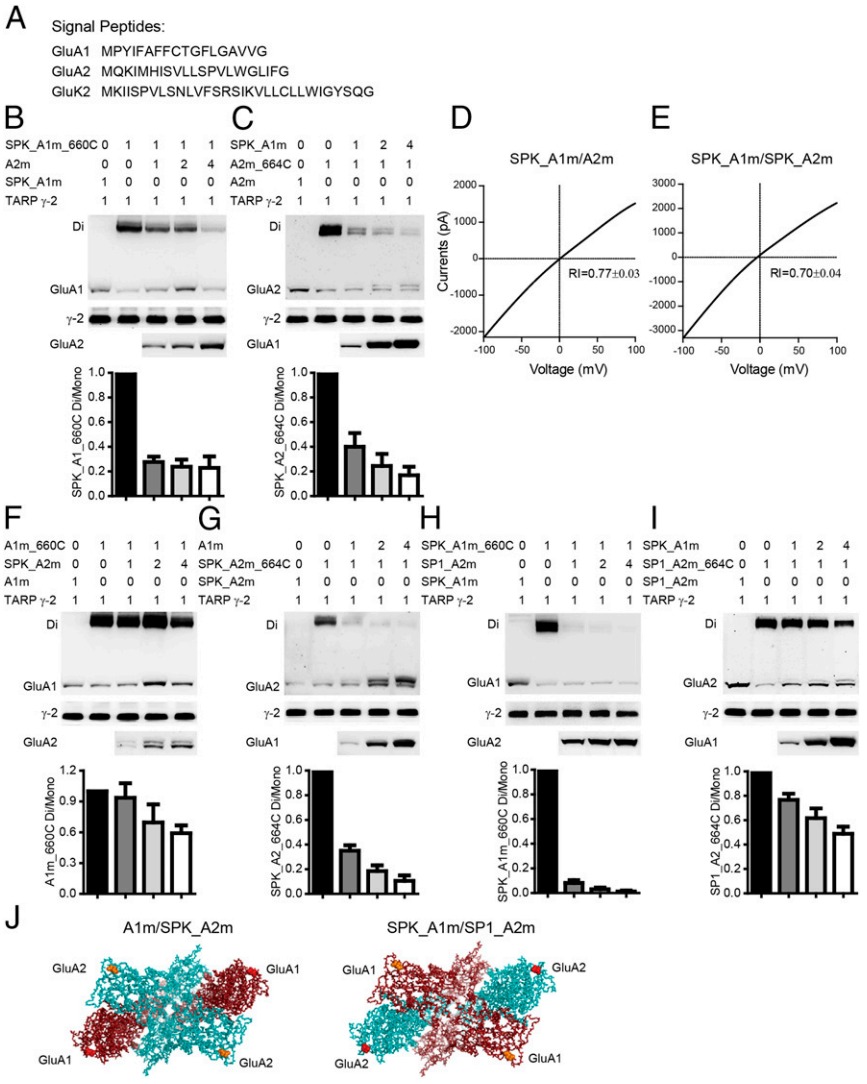

Fig. 6. GluA1 SP determines the heteromeric AMPAR assembly. (*A*) Sequences of SPs from GluA1, GluA2, and GluK2 receptors. (*B*) The dimer band of SPK_A1m_660C was greatly diminished when coexpressed with GluA2m. (*C*) The dimer band GluA2m_664C was greatly reduced when coexpressed with SPK_A1m. (*D* and *E*) The *I–V* curve of SPK_GluA1m/GluA2 (*D*) (n = 16) and SPK_GluA1m/SPK_GluA2 (*E*) (n = 20). (*F* and *G*) The dimer bands of GluA1m_660C were relatively stable when coexpressed with SPK_GluA2m (*F*), whereas the dimer bands of SPK_GluA2m_664C were greatly decreased with GluA1m (*G*). (*H* and *I*) The dimer bands of SPK_GluA1m_660C were greatly decreased when coexpressed with SP1_GluA2m (*H*), whereas the dimer bands of SP1_GluA2m_664C were relatively stable with SPK_GluA1m (*I*). (*J*) SP changed the architecture of GluA1/A2 (top view). The first amino acids were colored. The residues that link to GluA1, GluA2, and GluK2 SP are labeled in red, green, and yellow, respectively.

ATDs, they would have preferred to assemble into heterodimers at the first assembly step, as discussed. Then, they might further dimerize in a random manner so that the cross-linking bands are both decreased. The theoretical prediction of cross-linking patterns for this preferred heterodimer-random model is only slightly different from the complete random model, and our experimental data could not distinguish them from each other. A close comparison of the cross-linking pattern of GluA1/A2 with the 1–2–1–2 model showed that they are not strictly matched. The 1–2–1–2 model predicts that the dimers are constantly high when GluA1m_I660C is coexpressed with one to four times the GluA2m, yet a slight decrease of dimer bands was observed. The model also predicts that there are zero dimers when GluA2m_I664C is coexpressed with one to four times the GluA1m, yet small amounts of dimer bands have been observed. These observations suggest that GluA1/GluA2 stoichiometry might vary, so that 3:1 or 1:3 stoichiometry could form under certain conditions (14), although the 2:2 stoichiometry with the 1–2–1–2 architecture is highly preferred.

The elements controlling the second step of assembly, the dimerization of dimers, was previously unclear. A few sites—including the Lurcher site (alanine to threonine mutation) (11, 33), the R–Q RNA editing site (43), the flop-flip domains (44), and transmembrane domains (45)—have been suggested to affect the tetramerization step of the assembly, probably by changing the velocity of the second dimerization. Here, we clearly demonstrated that the GluA1 SP plays a critical role in determining the spatial arrangement of heteromeric receptor tetramerization. These results are rather surprising, because the SPs are generally cleaved off and degraded (34, 35) after guiding the newly synthesized peptides to enter the ER. Very few SPs are retained and have been implicated in protein function such as that of the secretory protein HRP (46). The maintained pseudo-SP of the membrane protein $CRF_{2(a)}R$ affects the receptor oligomerization (36, 47). In this study, SPs of GluA1 and GluA2 were cleaved off from the mature receptors (Fig. 5), suggesting that they belong to the traditional amino-terminal SPs. That a cleavable SP plays a role in late assembly of protein ternary structures, to our knowledge, has not been reported before, thus probably implying a novel function of SPs. Our finding also raises questions about when the SPs are excised. For GluA1/GluA2 receptors, a simple model would be that the SPs (at least the GluA1 SP) are cleaved off after the heterotetramer formation in the ER because the SPs have clearly *cis* effects on the spatial assembly. Alternatively, although less likely, the SPs are excised earlier, but have passed the spatial code to downstream signal molecules.

The SPs are not conserved, even between family proteins like AMPAR subunits. However, the SPs are conserved among species, including frog, turtle, chicken, and mammals, in either GluA1 or GluA2 (Fig. S10). This homogeneity of SPs among species

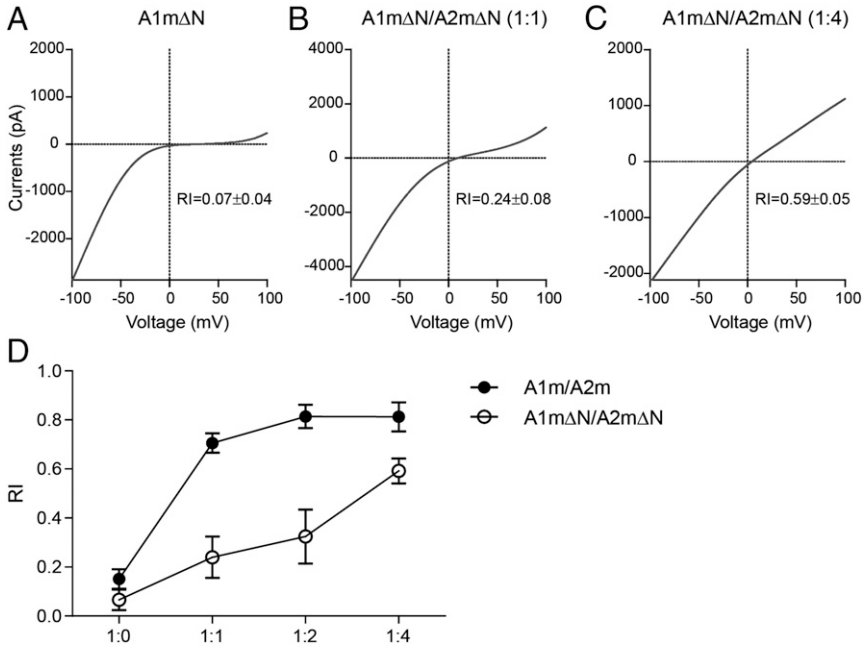

Fig. 7. The ATDs are critical for the heteromerization of GluA1/A2. (*A*) The glutamate current of GluA1mΔN was strongly rectified (n = 6). (*B*) The glutamate current of GluA1mΔN/GluA2mΔN (1:1) was partially rectified (n = 6). (*C*) *I–V* curve of GluA1mΔN/GluA2mΔN (1:4) was rather linear (n = 12). (*D*) Quantifications of RIs in *A–C*.

indicates that the AMPAR spatial assembly is evolutionally conserved.

Native AMPARs are modulated by auxiliary subunits in the brain. We and others have previously shown that one to four TARPs bind to each AMPAR (11, 15). By tethering TARP γ-2 or -8 with GluA1 and GluA2, we have determined that kainite- vs. glutamate-induced currents (KA/Glu ratio) are determined by the number of TARPs that are linked (15). Furthermore, coexpression of TARP-tethered GluA1 (or GluA2) with untethered GluA2 (or GluA1) showed an intermediate KA/Glu ratio, which can be best explained with two TARPs in each receptor. Regardless of the effects of TARPs on AMPAR assembly, the observation also suggests that GluA1/A2 form tetramers with 2:2 stoichiometry. Our data here show that TARP γ-2 does not alter the spatial assembly priority of heteromeric AMPARs, but, rather, enforces it. Assuming that almost all native AMPARs in neurons contain TARPs, the GluA1/A2 heteromeric AMPARs in the brain might have fixed stoichiometry and architecture.

In conclusion, our results suggest that GluA1/A2, the most abundant AMPARs in the brain, prefer to assemble into heterotetramers in a 1–2–1–2 fashion. This spatial assembly is determined by the SP of GluA1.

Methods

Protein Modeling. Protein sequences corresponding to rat GluA1 and GluA2 were downloaded from the UniProt database. These sequences were subsequently aligned to the sequence of the crystal structure (PDB ID 3KG2) by using BLAST. GluA1 and GluA2 sequences were, respectively, 71% and 97% identical to the 3KG2 sequence. We used the protein homology modeling program Protein Local Optimization Program (now commercially available as PRIME; Schrodinger, Inc.) to build the models (48). We modeled each protein chain separately and merged them together to construct the heterotetramer GluA1/A2 models. The models were depicted by using the PyMOL program.

Molecular Biology. The full-length rat GluA2 (flip) and TARP γ-2 subunits were subcloned into the pIRES2-GFP vector, and rat GluA1 (flip) were in pIRES2-mCherry vector for expression in HEK 293T cells (15). Single or multiple cysteine substitutions and the Q/R editing site were generated by using overlapping PCR (Vazyme Biotech, P505). To make constructs of GluA1 and GluA2 amino-terminal chimeras, the amino termini of GluA1 (397 residues including SP) and GluA2 (402 residues including SP) were exchanged by overlapping PCR. To make constructs of GluA1 and GluA2 SP chimeras, the SPs of GluA1 (18 residues), GluA2 (21 residues), and rat GluK2 were exchanged by overlapping PCR. Constructs with mutant codons were confirmed by sequencing over the entire length of the coding region.

Western Blots for Cysteine Cross-Linking. For AMPAR cross-linking experiments, HEK 293T cells were transiently transfected by using Lipofectamine 2000 reagent (Invitrogen) following the manufacturer's instructions. After 4 h, DNA–Lipofectamine 2000 complexes were removed by changing culture medium containing 100 μM 6-nitro-7-sulfamoylbenzo[*f*]quinoxaline-2,3-dione (Abcam). After 2 d, cells were either performed recording or lysed in radioimmunoprecipitation assay buffer containing 150 mM NaCl, 50 mM Tris (pH 7.4), 1% Nonidet P-40, 0.5% sodium deoxycholate, and complete Protease Inhibitor Mixture Tablets (Roche). Lysis was performed on ice for 30 min, and cell lysates were centrifuged for 30 min at 17,000 × *g* in a top bench centrifuge at 4 °C. After centrifugation, the supernatant was mixed with 4× loading buffer and immediately loaded into 6% SDS/PAGE gels in the absence (nonreducing condition) or presence of DTT. Protein bands were transferred to PVDF membranes (EMD Millipore) at 75 V for 3 h. The membranes were blocked for 1 h at room temperature in 150 mM NaCl, 10 mM Tris·HCl, pH 7.6, and 0.1% Tween 20 containing 5% nonfat milk and then probed with anti-GluA1 antibody (Abcam, catalog no. ab31232), anti-GluA2/3 antibody (Millipore, AB1506), or anti-Stargazin antibody (EMD Millipore, catalog no. AB9876). The protein detection was performed by using the ECL substrate (Thermo Fisher Scientific Life Sciences) before exposure.

Membrane Protein Extraction. Cells were washed three times with ice-cold PBS before adding 1 mM solution of Sulfo-NHS-LC-Biotin (Thermo Fisher Scientific Life Sciences, catalog no. 21335) in PBS for biotinylating cell surface proteins. The cells were incubated by reacting on ice for 30 min. Reactions were quenched with 50 mM glycine, followed by rinsing three times with ice-cold Tris-buffered saline. Cells were then lysed by sonicating in 0.5% Triton X-100 containing lysis buffer (with protease inhibitors) on ice. After centrifuging cell lysate at 13,800 × *g* for 10 min at 4 °C, clarified supernatants were transferred to monomeric avidin agarose (Thermo Fisher Scientific Life Sciences, catalog no. 20228). Incubation for 1 h at room temperature was performed, with end-over-end mixing for coupling biotinylated proteins to monomeric avidin agarose. The agarose was washed three times with PBS. Finally, the bound membrane proteins were eluted by incubating with nonreducing SDS/PAGE sample buffer containing 50 mM biotin at 70 °C for 10 min.

Electrophysiology. Agonist-evoked currents were recorded from transfected HEK 293T cells, as described (49). Patch-clamp recordings were performed 24–48 h after transfection in room temperature. The transfected HEK 293T cells were bathed in the extracellular solution containing the following (in mM): NaCl 150, KCl 2.8, $MgCl_2$ 0.5, $CaCl_2$ 2, and Hepes 10 (pH 7.4). Whole-cell patches were recorded from positively transfected cells identified by epifluorescence microscopy with glass pipettes (3–6 MΩ) filled with solution containing (in mM): CsF 110, CsCl 30, NaCl 4, $CaCl_2$ 0.5, EGTA 10, Hepes 10, and spermine 0.1 (pH 7.3) with CsOH. A concentration of 1 mM glutamate (and/or 10 mM DTT) was applied to patches in extracellular solution containing 0.5 mM TCM to prevent desensitization, at pH 7.4. All cells were voltage-clamped at −60 mV, and the current data were collected with an Axoclamp 700B amplifier and Digidata 1440A (Molecular Devices), filtered at 2 kHz, and digitized at 10 kHz. The patch data are analyzed by using Clampfit software.

Statistical Analysis. The ratio of dimers was quantified by using the image quantification software ImageJ. Data are expressed as mean ± SEM of at least three independent experiments. Statistical analyses were carried out by using GraphPad Prism software (Version 6). Specific tests used were multiple comparisons in one-way ANOVA and *t* test. All *P* values <0.05 were considered statistically significant.

ACKNOWLEDGMENTS. This work was initiated during the postdoctoral training of Y.S.S. in Prof. Roger A. Nicoll's laboratory at the University of California, San Francisco. We thank Prof. Nicoll for his generosity and thoughtful comments on the manuscript. This work is supported by National Basic Research Program of China Grants 2014CB942804 and 2015BAI08B00; National Science Foundation of China Grants 31371061, 31571060, 31500830, and 31200808; and Natural Science Foundation of Jiangsu Province Grant BK20140018.

1. Traynelis SF, et al. (2010) Glutamate receptor ion channels: Structure, regulation, and function. *Pharmacol Rev* 62(3):405–496.
2. Sommer B, Köhler M, Sprengel R, Seeburg PH (1991) RNA editing in brain controls a determinant of ion flow in glutamate-gated channels. *Cell* 67(1):11–19.
3. Cull-Candy S, Kelly L, Farrant M (2006) Regulation of Ca2+-permeable AMPA receptors: Synaptic plasticity and beyond. *Curr Opin Neurobiol* 16(3):288–297.
4. Jia Z, et al. (1996) Enhanced LTP in mice deficient in the AMPA receptor GluR2. *Neuron* 17(5):945–956.
5. Mansour M, Nagarajan N, Nehring RB, Clements JD, Rosenmund C (2001) Heteromeric AMPA receptors assemble with a preferred subunit stoichiometry and spatial arrangement. *Neuron* 32(5):841–853.
6. Burnashev N, et al. (1992) Calcium-permeable AMPA-kainate receptors in fusiform cerebellar glial cells. *Science* 256(5063):1566–1570.
7. Verdoorn TA, Burnashev N, Monyer H, Seeburg PH, Sakmann B (1991) Structural determinants of ion flow through recombinant glutamate receptor channels. *Science* 252(5013):1715–1718.
8. Hollmann M, Hartley M, Heinemann S (1991) Ca2+ permeability of KA-AMPA–gated glutamate receptor channels depends on subunit composition. *Science* 252(5007):851–853.
9. Lu W, et al. (2009) Subunit composition of synaptic AMPA receptors revealed by a single-cell genetic approach. *Neuron* 62(2):254–268.
10. Wenthold RJ, Petralia RS, Blahos J II, Niedzielski AS (1996) Evidence for multiple AMPA receptor complexes in hippocampal CA1/CA2 neurons. *J Neurosci* 16(6):1982–1989.
11. Kim KS, Yan D, Tomita S (2010) Assembly and stoichiometry of the AMPA receptor and transmembrane AMPA receptor regulatory protein complex. *J Neurosci* 30(3):1064–1072.
12. Rosenmund C, Stern-Bach Y, Stevens CF (1998) The tetrameric structure of a glutamate receptor channel. *Science* 280(5369):1596–1599.
13. Mano I, Teichberg VI (1998) A tetrameric subunit stoichiometry for a glutamate receptor-channel complex. *Neuroreport* 9(2):327–331.
14. Washburn MS, Numberger M, Zhang S, Dingledine R (1997) Differential dependence on GluR2 expression of three characteristic features of AMPA receptors. *J Neurosci* 17(24):9393–9406.
15. Shi Y, Lu W, Milstein AD, Nicoll RA (2009) The stoichiometry of AMPA receptors and TARPs varies by neuronal cell type. *Neuron* 62(5):633–640.
16. Dürr KL, et al. (2014) Structure and dynamics of AMPA receptor GluA2 in resting, pre-open, and desensitized states. *Cell* 158(4):778–792.
17. Chen L, Dürr KL, Gouaux E (2014) X-ray structures of AMPA receptor-cone snail toxin complexes illuminate activation mechanism. *Science* 345(6200):1021–1026.
18. Sobolevsky AI, Rosconi MP, Gouaux E (2009) X-ray structure, symmetry and mechanism of an AMPA-subtype glutamate receptor. *Nature* 462(7274):745–756.
19. Lee CH, et al. (2014) NMDA receptor structures reveal subunit arrangement and pore architecture. *Nature* 511(7508):191–197.
20. Kumar J, Schuck P, Mayer ML (2011) Structure and assembly mechanism for heteromeric kainate receptors. *Neuron* 71(2):319–331.
21. Das U, Kumar J, Mayer ML, Plested AJ (2010) Domain organization and function in GluK2 subtype kainate receptors. *Proc Natl Acad Sci USA* 107(18):8463–8468.
22. Kott S, Werner M, Körber C, Hollmann M (2007) Electrophysiological properties of AMPA receptors are differentially modulated depending on the associated member of the TARP family. *J Neurosci* 27(14):3780–3789.
23. Schwenk J, et al. (2009) Functional proteomics identify cornichon proteins as auxiliary subunits of AMPA receptors. *Science* 323(5919):1313–1319.
24. Shanks NF, et al. (2012) Differences in AMPA and kainate receptor interactomes facilitate identification of AMPA receptor auxiliary subunit GSG1L. *Cell Reports* 1(6):590–598.
25. Schwenk J, et al. (2012) High-resolution proteomics unravel architecture and molecular diversity of native AMPA receptor complexes. *Neuron* 74(4):621–633.
26. von Engelhardt J, et al. (2010) CKAMP44: a brain-specific protein attenuating short-term synaptic plasticity in the dentate gyrus. *Science* 327(5972):1518–1522.
27. Kalashnikova E, et al. (2010) SynDIG1: An activity-regulated, AMPA- receptor-interacting transmembrane protein that regulates excitatory synapse development. *Neuron* 65(1):80–93.
28. Tomita S, et al. (2003) Functional studies and distribution define a family of transmembrane AMPA receptor regulatory proteins. *J Cell Biol* 161(4):805–816.
29. Jackson AC, Nicoll RA (2011) The expanding social network of ionotropic glutamate receptors: TARPs and other transmembrane auxiliary subunits. *Neuron* 70(2):178–199.
30. Leuschner WD, Hoch W (1999) Subtype-specific assembly of alpha-amino-3-hydroxy-5-methyl-4-isoxazole propionic acid receptor subunits is mediated by their N-terminal domains. *J Biol Chem* 274(24):16907–16916.
31. Rossmann M, et al. (2011) Subunit-selective N-terminal domain associations organize the formation of AMPA receptor heteromers. *EMBO J* 30(5):959–971.
32. Ayalon G, Segev E, Elgavish S, Stern-Bach Y (2005) Two regions in the N-terminal domain of ionotropic glutamate receptor 3 form the subunit oligomerization interfaces that control subtype-specific receptor assembly. *J Biol Chem* 280(15):15053–15060.
33. Ayalon G, Stern-Bach Y (2001) Functional assembly of AMPA and kainate receptors is mediated by several discrete protein-protein interactions. *Neuron* 31(1):103–113.
34. Rutz C, Klein W, Schülein R (2015) N-terminal signal peptides of G protein-coupled receptors: Significance for receptor biosynthesis, trafficking, and signal transduction. *Prog Mol Biol Transl Sci* 132:267–287.
35. Hegde RS, Bernstein HD (2006) The surprising complexity of signal sequences. *Trends Biochem Sci* 31(10):563–571.
36. Rutz C, et al. (2006) The corticotropin-releasing factor receptor type 2a contains an N-terminal pseudo signal peptide. *J Biol Chem* 281(34):24910–24921.
37. Tomita S, Shenoy A, Fukata Y, Nicoll RA, Bredt DS (2007) Stargazin interacts functionally with the AMPA receptor glutamate-binding module. *Neuropharmacology* 52(1):87–91.
38. Pasternack A, et al. (2002) Alpha-amino-3-hydroxy-5-methyl-4-isoxazolepropionic acid (AMPA) receptor channels lacking the N-terminal domain. *J Biol Chem* 277(51):49662–49667.
39. Jin R, et al. (2009) Crystal structure and association behaviour of the GluR2 amino-terminal domain. *EMBO J* 28(12):1812–1823.
40. Sukumaran M, et al. (2011) Dynamics and allosteric potential of the AMPA receptor N-terminal domain. *EMBO J* 30(5):972–982.
41. Kumar J, Schuck P, Jin R, Mayer ML (2009) The N-terminal domain of GluR6-subtype glutamate receptor ion channels. *Nat Struct Mol Biol* 16(6):631–638.
42. Gan Q, Salussolia CL, Wollmuth LP (2015) Assembly of AMPA receptors: Mechanisms and regulation. *J Physiol* 593(1):39–48.
43. Greger IH, Khatri L, Kong X, Ziff EB (2003) AMPA receptor tetramerization is mediated by Q/R editing. *Neuron* 40(4):763–774.
44. Penn AC, Balik A, Wozny C, Cais O, Greger IH (2012) Activity-mediated AMPA receptor remodeling, driven by alternative splicing in the ligand-binding domain. *Neuron* 76(3):503–510.
45. Gan Q, Dai J, Zhou HX, Wollmuth LP (2016) The transmembrane domain mediates tetramerization of α-amino-3-hydroxy-5-methyl-4-isoxazolepropionic acid (AMPA) receptors. *J Biol Chem* 291(12):6595–6606.
46. Harrington JM, et al. (2014) A retained secretory signal peptide mediates high density lipoprotein (HDL) assembly and function of haptoglobin-related protein. *J Biol Chem* 289(36):24811–24820.
47. Teichmann A, et al. (2012) The pseudo signal peptide of the corticotropin-releasing factor receptor type 2A prevents receptor oligomerization. *J Biol Chem* 287(32):27265–27274.
48. Jacobson MP, Friesner RA, Xiang Z, Honig B (2002) On the role of the crystal environment in determining protein side-chain conformations. *J Mol Biol* 320(3):597–608.
49. Herring BE, et al. (2013) Cornichon proteins determine the subunit composition of synaptic AMPA receptors. *Neuron* 77(6):1083–1096.